J. Civil Eng. Mater.App. 2025 (March); 9(1): 35-45

Journal of Civil Engineering and Materials Application

Journal home page: http://jcema.com

Received: 04 January 2025 • Revised: 19 February 2025 • Accepted: 17 March 2025

Research

doi: 10.22034/jcema.2025.227518

Seismic Vulnerability Assessment of Low, Mid, and High-Rise RC Buildings Subjected to Near-Fault Earthquakes Using Fragility Curves

Navid Khedernejad *, Mohammad Keyvan Latifi

Department of Structural Engineering, Kurdistan Province Construction Engineering Organization-Iran.

*Correspondence should be addressed to Navid Khedernejad, Kurdistan Province Construction Engineering Organization-Iran.; Email: navidinter@gmail.com

ABSTRACT

In this study, seismic vulnerability fragility curves were developed for special RC moment-resisting frames with 3, 7, and 15 stories, corresponding to low-, mid-, and high-rise buildings as defined by the HAZUS-MH 2.1 guidelines. The 2D frames were modeled and analyzed using nonlinear time history analysis in OpenSees software, subjected to 14 near-fault ground motion records. The interstory drift ratio was considered as the damage index. The drift limits specified in the HAZUS guidelines were used to define slight, moderate, extensive, and complete damage states based on the structural system type and the number of stories, in order to generate fragility curves. The analytical and numerical investigations revealed that, in the 3-story frame, the increase in damage levels relative to the slight damage level was 1.76, 4.71, and 14.58 times for moderate, extensive, and complete damage levels, respectively. For the 7-story frame, these increases were 0.98, 5.36, and 11.37 times, while for the 15-story frame, the corresponding values were 1.2, 2.34, and 7.46 times, respectively. Overall, it can be concluded that with an increase in the number of stories and Peak Ground Acceleration (PGA), seismic fragility increases. However, the 15-story frame exhibited the least probability of complete damage compared to the 7- and 3-story frames, whereas the 3-story frame experienced the highest likelihood of slight damage among all.

Keywords: RC Moment Frames, Time History Analysis, Near-Fault Earthquake, Fragility Curves

1. INTRODUCTION

The investigation of structural behavior in various seismically active cities has always been one of the fundamental issues in earthquake engineering. With the advancement of modern seismic analysis methods and the increasing use of performance-based seismic design of structures, the necessity to evaluate buildings designed according to national design codes has become evident [1]. In recent years, seismic vulnerability assessment methodologies have increasingly relied on fragility curves as an effective tool for

structural vulnerability evaluation. Fragility curves represent the probability that the seismic demand on a structure exceeds its capacity with respect to a ground motion intensity parameter. The development of these curves initially focused on nuclear facilities, as these structures are critically important, and their damage during earthquakes can lead to severe environmental disasters. The first fragility curve for a nuclear power plant was developed in Japan in 1980. Fragility curves provide quantitative information regarding damage states and earthquake characteristics to designers. Establishing the relationship between earthquake intensity and damage level is an essential tool for estimating building damage at an urban scale.

In recent years, the seismic behavior of reinforced concrete structures under various earthquake events, as well as the assessment of their seismic vulnerability, has been the subject of numerous investigations worldwide. One of the key tools in seismic vulnerability assessment is the fragility curve, which represents the probability that the structural damage will exceed a specified seismic damage state for multiple levels of ground motion intensity.

In 2012, Shabakhti and colleagues investigated the seismic vulnerability of dual systems composed of steel moment-resisting frames and shear walls by developing fragility curves [2]. In 2014, Hamidi and colleagues selected a medium-rise reinforced concrete building designed according to the first edition of the Iranian Standard 2800, which was considered vulnerable based on existing seismic retrofit guidelines. For seismic rehabilitation, an X-bracing system was implemented, applying one of three different spatial distributions to the structure. A comparison between the seismic performance levels of the original and retrofitted structures was conducted using fragility curves. Time-history analyses were performed with 12 near-fault earthquake ground motion records. The intensity measure considered was PGA (peak ground acceleration), and the damage index was the axial plastic hinge failure. Using a lognormal distribution, seismic fragility curves were developed and compared [3]. In 2014, Ghodrati Amiri and colleagues conducted a seismic assessment of typical masonry school buildings in Iran using fragility curves. Employing an analytical approach, they developed separate fragility curves for masonry buildings with one, two, and three stories, considering the different soil types specified in Standard No. 2800 [4]. In 2015, Doosti and colleagues, after explaining the fundamental concepts of fragility curves, provided a comprehensive overview of the methods used for their development. Accordingly, they identified four principal approaches: empirical, expert judgment-based, analytical, and hybrid. They noted that analytical methods are the most commonly employed approach in the technical literature [5]. In 2016, Enayati Abar and Fallahi investigated the seismic vulnerability fragility curves of medium-ductility reinforced concrete moment-resisting frame systems designed in accordance with the Iranian seismic code, in regions with very high seismic hazard. Their results indicated that the probability of collapse for the 4-story and 7-story models at the design basis acceleration specified by Standard No. 2800 for very high seismic hazard zones was close to zero, demonstrating the excellent performance of such structures against the design basis earthquake [6]. In 2017, Amiri and colleagues selected three types of reinforced concrete buildings with identical floor plans consisting of 3, 5, and 8 stories. These structures were retrofitted using steel eccentrically braced frames with vertical links. Subsequently, they performed seismic evaluation by modeling the buildings in OpenSees software, applying nonlinear dynamic analysis, and developing fragility curves [7]. In 2017, Noori and colleagues investigated the effect of uncertainty in earthquake incidence angle on the increased engineering demand parameters of large highway bridge components. To this end,

nonlinear dynamic analyses were performed using 80 ground motion records (40 near-fault and 40 far-fault) applied from 12 different directions ranging from 0 to 180 degrees on numerical models of bridges with skew angles varying from 0 to 60 degrees. Fragility curve components were developed, and the results were compared with analyses considering earthquakes applied only along the principal directions [8]. In 2018, Yousefzadeh and colleagues investigated the effect of connection regions in moment-resisting frames with bolted flange plate connections and reduced section connections for two sets of 4- and 16-story frames under near-field earthquake motions. They performed incremental nonlinear dynamic analyses and compared the results using fragility curves. Based on the fragility curves, it was observed that employing the stiffest connection springs allowed by the code yields the best seismic performance outcomes [9]. In 2019, Alizadeh Kashani and colleagues examined the fragility curves of asymmetric structures using the multiple strip method. They studied a 9-story 3D SAC building with no mass asymmetry and with 10%, 15%, and 20% mass asymmetry. The selected structure was subjected to 200 earthquake records, and the maximum inter-story drift as well as the spectral acceleration at the dominant mode period were calculated. To assess seismic damage, fragility curves were developed, analyzed, and compared. The results indicated an increased probability of collapse with greater mass eccentricity and structural asymmetry up to a certain seismic intensity level [10]. In 2020, Baharloo and colleagues evaluated the vulnerability of structures retrofitted at different strengthening levels compared to the original weak structures. Their analyses on 5-, 8-, and 15-story buildings showed that the use of CFRP sheets is generally more economical. However, since shear walls significantly reduce the probability of exceeding the collapse threshold at high seismic intensities, the benefit-to-cost ratios of the two methods become comparable in taller, more vulnerable buildings [11]. In 2020, Gorji and colleagues examined the impact of significant inherent and epistemic uncertainties on the seismic performance of medium-rise steel moment-resisting frames. For this evaluation, they employed the generalized incremental dynamic analysis (IDA) method [12]. In 2021, Daneshjoo and colleagues proposed an appropriate methodology for generating analytical seismic fragility curves of steel frames. They recommended that, in order to estimate the probability of exceedance of performance levels, a probabilistic assessment should be conducted prior to fragility analysis. This involves applying goodness-of-fit tests to identify the best-fitted probability distribution at each performance level, after which the structural vulnerability can be estimated using the derived fragility curves [13]. In 2024, Heydari and Emami developed seismic fragility curves for reinforced concrete school buildings in Isfahan Province. The fragility curves were generated considering the spectral acceleration at the fundamental period with 5% damping as the intensity measure, and the maximum inter-story drift ratio as the damage index. Their findings revealed that the probability of exceedance in buildings located in moderate seismic hazard zones is higher than that in regions with high seismic hazard [14]. In 2024, Asadi and Abbasi applied the proposed method to develop fragility curves for three steel structures. They demonstrated that, compared to the conventional Monte Carlo approach, the fragility curves could be generated using fewer analyses, while achieving lower errors than those obtained from other existing methods [15]. In 2024, Razmkhah and colleagues investigated the damage caused by the combined effects of corrosion, aftershocks, and the damage induced by the main earthquake, utilizing fragility curves to quantify the structural vulnerability [16].

2. METHODOLOGY

2.1. Structural Model System

Three special RC moment-resisting frames with 3, 7, and 15 stories—each consisting of three 6-meter bays and a story height of 3.2 meters—were initially modeled, analyzed, and designed using ETABS software. The designed frame sections were then modeled and analyzed in the OpenSees finite element software to perform nonlinear time history analysis.

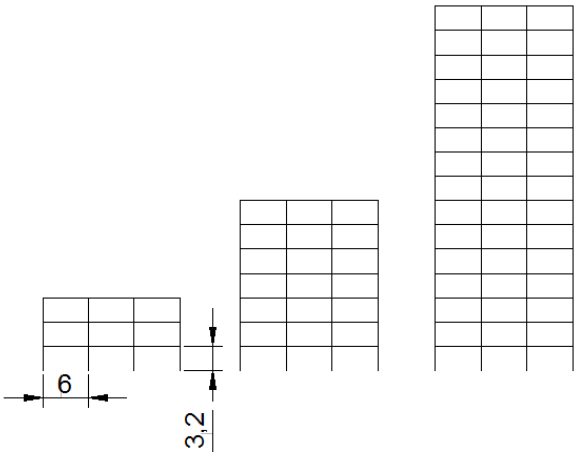

Figure 1. Illustrates the three-bay moment-resisting frames with 3,7 and 15 stories

Table 1. The structural sections designed for the 3-,7- and 15-story frames are listed below

All beams have a cross-section of 40×45cm with 4T20 top and 4T20 bottom longitudinal reinforcement.				**The 3-story frames**
Story	Cross-section of the corner columns	Reinforcement of the corner columns	Cross-section of the interior columns	**Reinforcement of the interior columns**
1st	45 x 45	12 T 22	45 x 45	**12 T 22**
2nd	45 x 45	12 T 18	45 x 45	**12 T 18**
3rd	40 x 40	10 T 16	40 x 40	**10 T16**
All beams have a cross-section of 45×55cm with 4T22 top and 4T22 bottom longitudinal reinforcement.				**The 7-story frames**
Story	Cross-section of the corner columns	Reinforcement of the corner columns	Cross-section of the interior columns	**Reinforcement of the interior columns**
1st	60 x 60	16 T 22	60 x 60	**16 T 22**
2nd	60 x 60	16 T 22	60 x 60	**16 T 22**
3rd	55 x 55	16 T 20	55 x 55	**16 T 20**
4th	55 x 55	16 T 20	55 x 55	**16 T 20**
5th	50 x 50	12 T 20	50 x 50	**12 T 20**
6th	50 x 50	12 T 20	50 x 50	**12 T 20**
7th	45 x 45	12 T 18	45 x 45	**12 T 18**
Cross-section of all beams in floors 1 to 6		50 X 60cm – 5T22 top and 5T22 bot		**The 15-story frames**
Cross-section of all beams in floors 7 to 15		45 X 55cm – 4T22 top and 4T22 bot		
Story	Cross-section of the corner columns	Reinforcement of the corner columns	Cross-section of the interior columns	**Reinforcement of the interior columns**
1st	60 x 60	16 T 28	70 x 70	**20 T 28**
2nd	60 x 60	16 T 28	70 x 70	**20 T 28**
3rd	55 x 55	16 T 22	70 x 70	**20 T 28**
4th	55 x 55	16 T 22	70 x 70	**20 T 28**
5th	50 x 50	12 T 22	70 x 70	**20 T 28**
6th	50 x 50	12 T 22	70 x 70	**20 T 28**
7th	45 x 45	12 T 22	55 x 55	**12 T 28**
8th	45 x 45	12 T 22	55 x 55	**12 T 28**
9th	45 x 45	12 T 22	55 x 55	**12 T 28**
10th	45 x 45	12 T 22	45 x 45	**12 T 22**
11th	45 x 45	12 T 22	45 x 45	**12 T 22**

12th	45 x 45	12 T 22	45 x 45	**12 T 22**
13th	45 x 45	12 T 22	45 x 45	**12 T 22**
14th	45 x 45	12 T 22	45 x 45	**12 T 22**
15th	45 x 45	12 T 22	45 x 45	**12 T 22**

2.2. Element and Section Formulation

In both beam and column elements, the disp Beam Column element defined in the OpenSees library was used. In this study, the fiber Section approach was adopted for section modeling. The fiber model is based on distributed plasticity formulations. The fiber-based modeling approach is considered one of the most reliable formulations for predicting the seismic response of structural systems, due to its ability to localize the spread of plasticity to specific regions of a section rather than over the entire section. In this study, five integration points were assigned to each beam and column element.

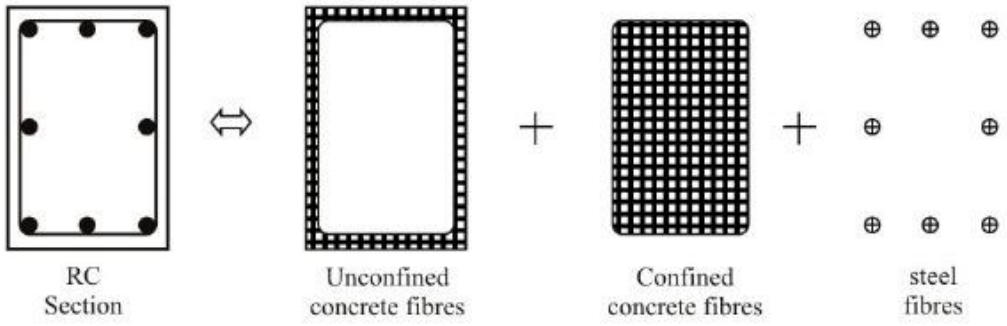

Figure 2. Fiber Modeling Approach for Reinforced Concrete Sections

2.3. Definition of Material Constitutive Models Using the Finite Element Method

To enhance the accuracy of the structural analysis results, materials capable of being modeled using the finite element method are utilized. The materials and elements used for this type of modeling are introduced in the following sections:

Reinforced concrete: Concrete is defined using the Concrete02 material model, which was developed by Hescham and Yassin [17]. This command is used to create a concrete material that accounts for the tensile region and includes linear softening behavior in tension. The Concrete02 material requires the following input parameters in order:

- 28-day compressive strength of concrete
- Corresponding strain at that compressive strength
- Crushing (ultimate) strength of concrete
- Strain at crushing strength
- Unloading/reloading stiffness ratio (slope)
- Maximum tensile strength of concrete
- Tensile softening stiffness

The figure below shows the stress-strain behavior of concrete based on the selected material model.

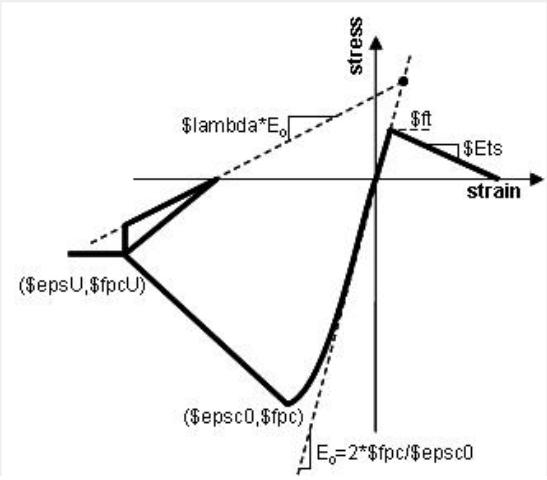

Figure 3. Stress-Strain Diagram of Concrete02 Material

The Steel02 material model, developed by Filippou et al. [18], was used for modeling steel. In this material definition, after specifying the tag number, the following parameters are provided to the software in order:

•Yield stress

•Elastic modulus (Young's modulus)

•Strain hardening ratio

•Parameter defining the curvature between the initial and secondary slopes of the steel's stress-strain behavior

The stress–strain behavior of this material as implemented in OpenSees is illustrated in the figure below.

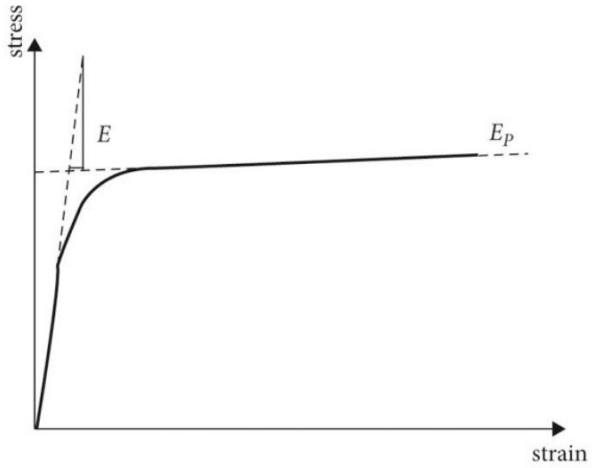

Figure 4. Stress-Strain Diagram of Steel Material

2.4. Loading

In the floors, the dead load of the floors plus the dead load of partition walls without any factor and the live load with a factor of 0.2 are considered. On the roof, the dead load of the roof plus the dead load of the walls without any factor and the live load of the roof with a factor of 0.2 are considered. For loading these frames, the dead loads of the floors and roof are considered as 450 kg/m² and 500 kg/m², respectively; the live loads of the floors and roof are considered as 200 kg/m² and 150 kg/m², respectively; and the partition wall load is taken as 100 kg/m².

Table 2. Fundamental Periods of the Designed Frames in ETABS and Comparison with OpenSees Models

	Three-Story Frame	Seven-Story Frame	Fifteen-Story Frame
1st Mode Period in Etabs	0.566 Sec	0.907 Sec	**1.885 Sec**
1st Mode Period in OpenSees	0.561 sec	0.892 Sec	**1.832 Sec**

2.5. Selection of Earthquake Records

Near-fault earthquake records were used for nonlinear time history analyses. The stability margin and load-bearing capacity of structures located in the near-fault zone are critically important due to the nature of near-fault earthquakes, which impose high lateral forces on the structure within a short duration. Therefore, different design considerations and approaches are necessary for these structures compared to those situated far from the fault zone. Near-fault ground motion records typically have shorter duration and significantly larger vertical components, whereas far-field ground motions generally exhibit longer durations with negligible vertical components. Near-fault records are characterized by high accelerations with a rich high-frequency content compared to far-field components, and they often contain a distinct initial pulse at the beginning of the record. The distance from the fault zone is a critical factor in selecting ground motions, as it can lead to substantially different structural responses. There is some variation in the literature regarding the exact cutoff distance distinguishing near-fault from far-field ground motions. FEMA P-695 considers the

distance from the fault as the basis for defining near- and far-field classifications. Based on a review of various references, it is generally accepted that if a ground motion is recorded at a station located less than 10 kilometers from the fault, it is definitively classified as a near-fault record. Distances greater than 20 kilometers are considered far-field zones, while distances between 10 and 20 kilometers require further evaluation based on the shape of the record and the vertical component of the earthquake to categorize them as near- or far-field. According to the recommendations of Shome and Cornell, selecting 10 to 20 ground motion records provides acceptable accuracy for estimating seismic demand [19]. In this study, 14 records from global earthquakes have been selected. The details of these selected earthquakes are listed in the table below.

Table 3. Characteristics of the selected Earthquakes

Earthquake	Year	Magnitude (Richter)	Station	Vs (m/s)	R (km)	(PGA max) g
Cape Mendocino	1992	7.01	Petrolia	422.17	0.0	**0.6615637**
Chi-Chi Taiwan	1999	7.62	Tcu065	305.85	0.57	**0.789778**
Chi-Chi Taiwan	1992	7.62	Tcu102	714.27	1.49	**0.3039302**
Duzce , Turkey	1999	7.14	Bolu	293.57	12.02	**0.8056801**
Erzican, Turkey	1992	6.69	Erzincan	352.05	0.0	**0.4961846**
Imperial Valley-06	1979	6.53	El Centro Array#6	203.22	0.0	**0.4490432**
Imperial Valley-06	1979	6.53	El Centro Array#7	210.51	0.56	**0.4690871**
Irpinia,Italy-01	1980	6.90	Sterno(STN)	382	6.78	**0.320522**
Kocaeli , Turkey	1999	7.51	Izmit	811.0	3.62	**0.2301705**
Landers	1992	7.28	Lucerne	1369.0	2.19	**0.7887603**
Loma Prieta	1989	6.93	Saratoga-Aloha Ave	380.89	7.58	**0.5144551**
Northridge01	1994	6.69	Rinaldi Receiving Sta	282.25	0.0	**0.8740596**
Northridge01	1994	6.69	Sylmar-Olive	440.54	1.74	**0.843358**
Superstition Hills-02	1987	6.54	Parachute Test Site	348.69	0.95	**0.431817**

2.6. Index and Damage Levels

To assess the vulnerability of structures, it is necessary to define a damage index. Here, the inter-story drift is considered as the damage index. Different damage states are defined and evaluated based on the values of drift. Moreover, a set of damage states must be established so that the models under study can be assessed for seismic vulnerability by checking whether they reach these damage thresholds. In this study, the damage states defined in the Hazus – MH 2.1 guideline have been used. The damage states introduced in the Hazus guideline for special reinforced concrete moment frames with low, medium, and high numbers of stories consist of four damage levels based on the inter-story drift ratio:

- Slight Damage
- Moderate Damage
- Extensive Damage
- Complete (or Collapse) Damage

The numerical values corresponding to each damage state are presented in the table below.

Table 4. Inter-Story Drift Ratios for Each Damage State According to Hazus

Damage State	Low-Rise Special (RC) Moment Frame	Mid-Rise Special (RC) Moment Frame	High-Rise Special (RC) Moment Frame
(Slight)	0.0063	0.0042	**0.0031**
(Moderate)	0.0125	0.0083	**0.0063**
(Extensive)	0.0375	0.0250	**0.0188**
(Complete)	0.1000	0.0667	**0.0500**

2.7. Fragility Curves

Seismic fragility curves are assumed to follow a lognormal probabilistic distribution. To construct this distribution, only two parameters are required: the mean and the standard deviation. Once the mean and standard deviation for each limit state are determined, the fragility curves can be plotted using Equation (1). The fragility function in terms of mean spectral acceleration is expressed as follows:

$$F(S_a) = \Phi[\frac{1}{\beta_c} ln(\frac{S_a}{A_t})] \quad (1)$$

In this equation, Φ represents the standard lognormal cumulative distribution function. Sa denotes the spectral acceleration amplitude at a period of 1 second. Ai is the mean expected spectral acceleration corresponding to the occurrence of the i-th damage state. βc is the normalized composite lognormal standard deviation, which accounts for uncertainties including the randomness in both capacity and demand. Using the logarithmic mean and standard deviation obtained from different ground motion records, fragility curves are developed for each of the defined limit states.

2.8. General Steps for Developing Fragility Curves

•Design of Frame Sections in structural software such as ETABS

•Modeling of the Frames in OpenSees using the design results from the previous step

•Performing Nonlinear Time History Analyses in OpenSees

•Extracting Maximum Inter-Story Drift Ratios

•Conducting Statistical Analysis using the mathematical software EasyFit

•Plotting Fragility Curves based on two parameters: PGA (Peak Ground Acceleration) and Probability of Damage.

3. RESULTS AND DISCUSSION

3.1. Validation of global models

Figure 5 illustrates the fragility curves for the three-story special reinforced concrete (RC) moment frame. According to the plots shown in Figure 5, the PGA corresponding to the onset of slight damage in this set of ground motions is 0.434g. The corresponding PGAs for other performance levels are:

- Moderate Damage: 0.764g
- Extensive Damage: 2.046g
- Complete Damage: 6.329g

Figure 6 shows the fragility curves for the seven-story special RC moment frame. Based on the curves presented in Figure 6, the PGA at the slight damage level is 0.391g. The PGAs for the other damage states are as follows:

- Moderate Damage: 0.687g
- Extensive Damage: 2.099g
- Complete Damage: 4.447g.

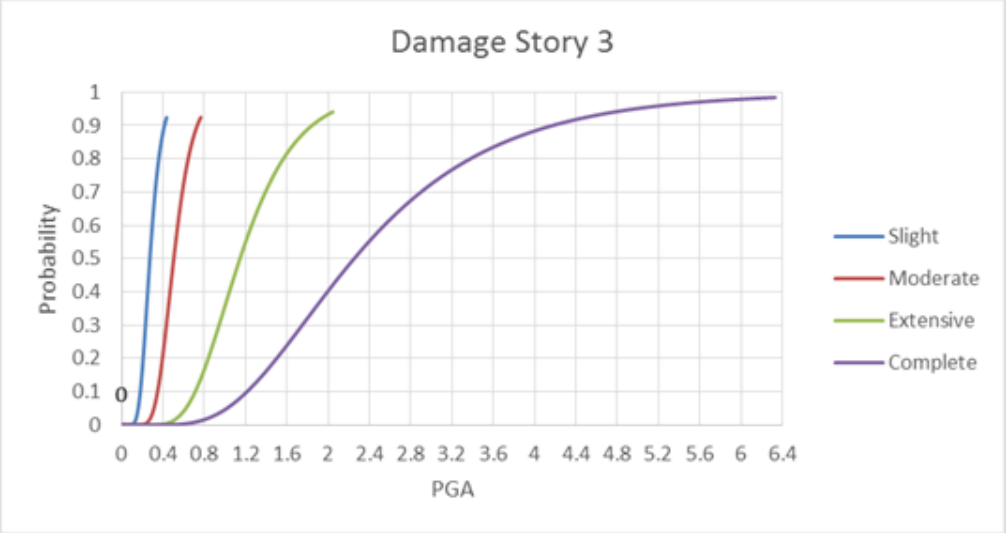

Figure 5. Fragility Curves for the 3-Story Special Reinforced Concrete Moment Frame

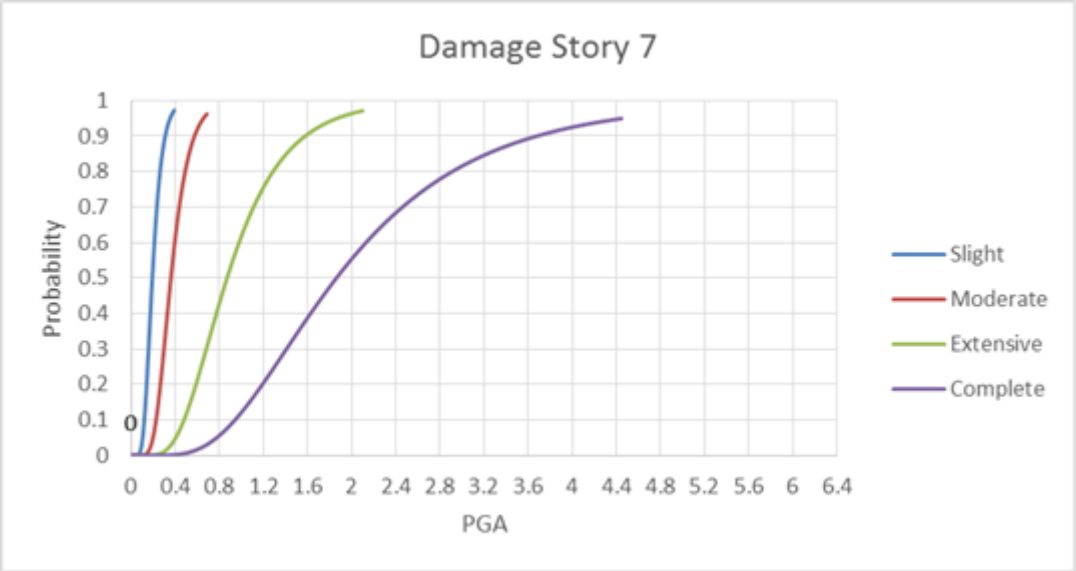

Figure 6. Fragility Curves for the 7-Story Special Reinforced Concrete Moment Frame

Figure 7 presents the fragility curves for the 15-story special reinforced concrete moment frame. According to the curves shown in Figure 7, the spectral acceleration (PGA) corresponding to the onset of slight damage in this set of ground motion records is 0.39g.

The corresponding PGAs for other damage states are as follows:

•Moderate Damage: 0.471g
•Extensive Damage: 0.913g
•Complete Damage: 2.91g

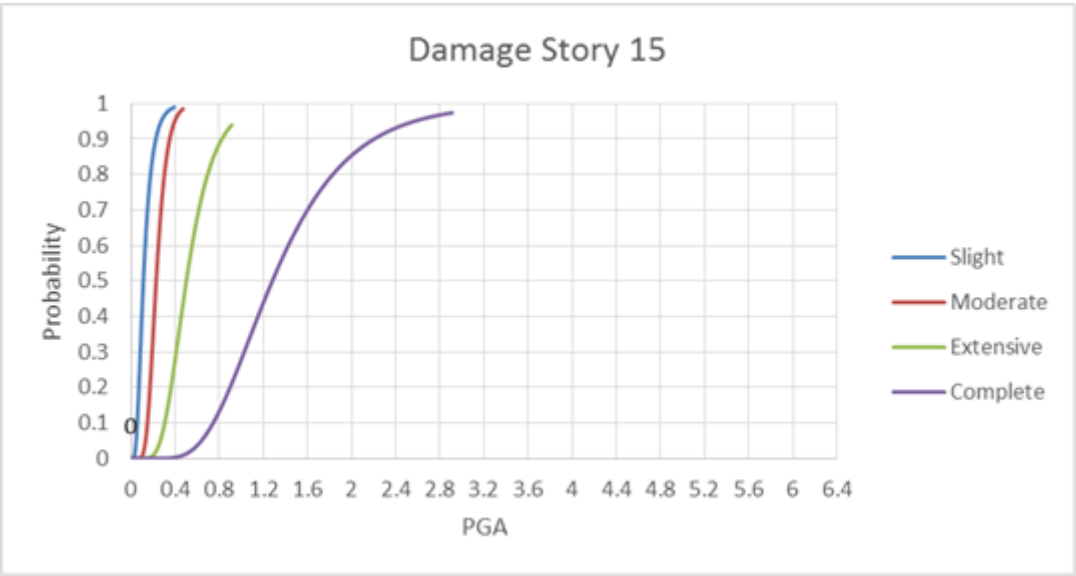

Figure 7. Fragility Curves for the 15 Story Special Reinforced Concrete Moment Frame

The following results can be observed from Figure 8. The 15-story frame exhibits greater resistance against complete damage and enters this stage at higher PGA values.

The 7-story frame demonstrates an intermediate behavior, showing greater vulnerability to extensive and complete failure compared to the 15-story frame, while being more resistant than the 3-story frame.

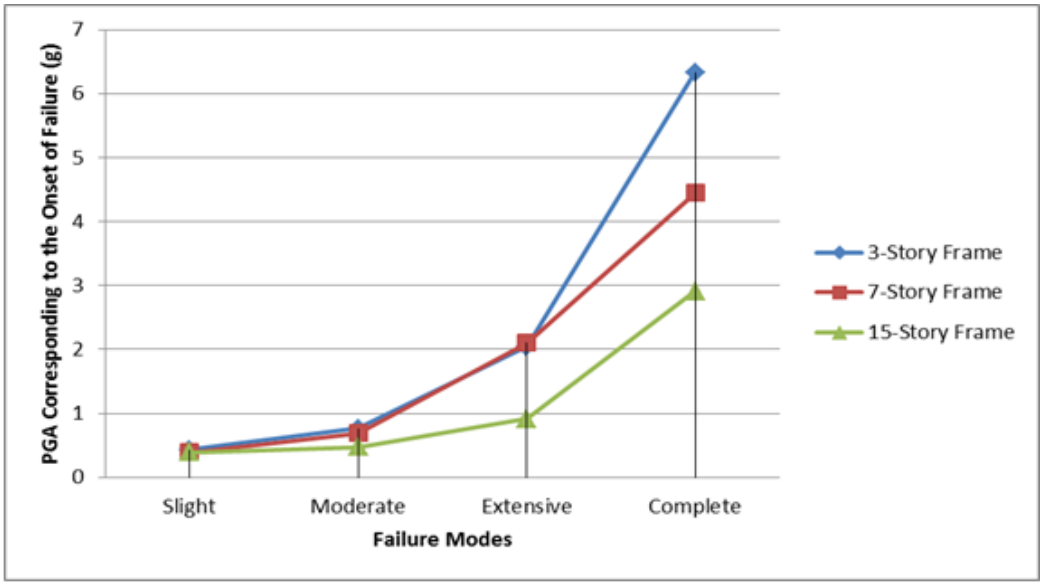

Figure 8. Comparison of PGA Values Corresponding to the Onset of Failure Modes in Different Frames

3.2. Influence of Building Height and Near-Field Ground Motions on Structural Vulnerability

Low-rise frames (three storeys) show the highest probability of slight damage. Their greater stiffness makes them more susceptible to excitation by ground motions with high-frequency content; even at relatively small peak ground acceleration (PGA) values, interstorey drifts can exceed permissible limits, initiating cracking and non-structural damage. By contrast, high-rise frames (fifteen storeys) tend to have a more uniform deformation profile along their height and higher ductility, which lowers the likelihood of reaching complete damage. As building height increases, damage progresses more gradually and collapse, if it occurs, does so at larger PGA levels.

Near-field earthquakes, characterized by early velocity pulses and high acceleration amplitudes over short durations, markedly influence structural response. Low-rise frames are particularly affected because their natural periods align more closely with the higher-frequency content typical of near-field records, increasing the likelihood of minor damage in three-storey systems. In high-rise structures, lower-frequency pulses can drive moderate to extensive damage; however, greater energy-absorption capacity generally prevents rapid progression to complete failure.

Mid-rise frames (seven storeys) are highly sensitive to both the velocity pulse and the broader frequency content of near-field motions. Their natural periods commonly fall in a range where both effects are significant. Consequently, the probability of extensive or complete failure in a seven-storey frame is higher than in a fifteen-storey frame but lower than in a three-storey frame.

From a design standpoint, low-rise buildings benefit from tighter control of interstorey drift to reduce premature damage. High-rise buildings require emphasis on ductility capacity and on measures that limit progressive collapse to avoid extensive or complete failure states. For mid-rise buildings, special attention to the effects of near-field velocity pulses is essential, as these structures are the most sensitive to this form of excitation.

4. CONCLUSION

In this study, seismic vulnerability fragility curves were developed for special reinforced concrete moment-resisting frames with 3, 7, and 15 stories, in accordance with the HAZUS-MH 2.1 guidelines, representing low-rise, mid-rise, and high-rise building categories, respectively. Based on the analysis of the models, the following conclusions can be drawn:

•In the 3-story reinforced concrete frame, the variation in performance levels relative to the slight damage state shows an increase by factors of approximately: 1.76 times for moderate damage, 4.71 times for extensive damage and 14.58 times for complete damage.

•In the 7-story reinforced concrete frame, the change in performance levels relative to the slight damage

state shows an increase by factors of approximately: 0.98 times for moderate damage, 5.36 times for extensive damage and 11.37 times for complete damage.

•In the 15-story reinforced concrete frame, the variation in performance levels relative to the slight damage state indicates an increase by factors of approximately: 1.20 times for moderate damage, 2.34 times for extensive damage and 7.46 times for complete damage.

The results indicated that the 15-story structure experienced less complete damage compared to the 7-story and 3-story structures. Additionally, the 3-story structure exhibited the highest level of slight damage among the three, compared to the 7-story and 15-story frames.

FUNDING/SUPPORT

Not mentioned any Funding/Support by authors.

ACKNOWLEDGMENT

Not mentioned any by authors.

AUTHORS CONTRIBUTION

This work was carried out in collaboration among all authors.

CONFLICT OF INTEREST

The author (s) declared no potential conflicts of interests with respect to the authorship and/or publication of this paper.

5. REFERENCES

[1] Nozafati Khameneh Y, Emami K, Saberi M. Fragility assessment of steel structures with medium moment frames using Incremental Dynamic Analysis (IDA). In 4th Conference on Construction and Project Management 2017. Tehran. [View at Publisher]

[2] Shabakhti N, Biyari M A. Seismic Vulnerability Assessment of Steel Dual Systems Consisting of Moment-Resisting Frames and Shear Walls with Development of Fragility Curves. In The 3rd National Conference on Structures and Steel and the 1st National Conference on Light Steel Structures 2011. Tehran. [View at Publisher]

[3] Hamidi H, Faghih-Maleki H, Gholampour S. Seismic Retrofit of Reinforced Concrete Structures Using Cross Bracing with the Presentation of Seismic Fragility Curves. In The 8th National Congress of Civil Engineering 2014. Babol: Noshirvani University of Technology. [View at Publisher]

[4] Ghodrati A G, et al. Analytical Fragility Curve Development for Masonry Buildings. In 8th Congress on Civil Engineering of Iran 2014. Babol. [View at Publisher]

[5] Doosti L, et al. Introduction and Review of Methods for Developing Fragility Curves. In 2nd National Conference on Structural Engineering of Iran 2015. Tehran: Iranian Society of Structural Engineering. [View at Publisher]

[6] Enayati Abr H, et al. Development of Seismic Fragility Curves for Reinforced Concrete Buildings with Intermediate Moment Resisting Frame Systems. In 9th National Congress on Civil Engineering 2016. [View at Publisher]

[7] Amiri M, et al. Seismic Retrofit of Reinforced Concrete Buildings Using Eccentrically Braced Frames with Vertical Links through the Development of Fragility Curves. In The 2nd National Conference on Applied Research in Civil Engineering 2017. [View at Publisher]

[8] Noori H, Memarpour M M, Yakhchalian M. Investigation of the Spatial Distribution of Earthquakes on Fragility Curves of Highway Bridge Components with Skewed Supports in Near- and Far-Fault Regions. Journal: Transportation Infrastructure Engineering, 2017; 3(2): 89–110. [View at Google Scholar]; [View at Publisher]

[9] Yousofzadeh M, et al. The effect of connection welds on the behavior of reduced-section connections and reduced-section connections using the bolted splice method on the fragility curve under near-fault earthquakes. In Conference on Civil Engineering, Architecture, and Urban Planning of Islamic Countries 2018. [View at Publisher]

[10] Kashani K H, et al. Development of Fragility Curves for Structures with Mass Irregularity Using the Multi-Strip Analysis Method. In The 3rd International Conference on Applied Research in Structural Engineering and Construction Management 2019. Tehran. [View at Publisher]

[11] Baharloo H, et al. Seismic Vulnerability Assessment of Deficient Reinforced Concrete Frames Retrofitted Using Different Methods and Levels Based on Fragility Curves and Cost-Benefit Analysis. Journal: Earthquake Science and Engineering, 2020; 22(1). [View at Publisher]

[12] Gorji A H, et al. Investigation of Aleatory and Epistemic Uncertainties in the fragility curves of steel moment–resisting frame systems. Journal: Civil Engineering, 2020; 33(3). [View at Google Scholar]; [View at Publisher]

[13] Daneshjo F, et al. Development of Seismic Fragility Curves for High-Rise Structures and Proposing a Method for Selecting the Optimal Probability Distribution Function at Different Performance Levels. Journal: Modares Civil Engineering Journal, 2021; 22(2). [View at Google Scholar]; [View at Publisher]

[14] Heydari A, et al. Development of Seismic Fragility Curves for Reinforced Concrete School Buildings in Isfahan Province. In The 9th International Conference on Seismology and Earthquake Engineering 2024. Tehran: IIEES. [View at Google Scholar]; [View at Publisher]

[15] Asadi P, Abbasi H. Fragility curves production for steel structures by seismic improvement of the high-dimensional model representation method. Journal: Omran Sharif Journal, 2024; 40(1): 65–76. [View at Google Scholar]; [View at Publisher]

[16] Razmkhah M, et al. Assessment of the Fragility Curve of Low-Rise Steel Moment-Resisting Frames under Corrosion and Aftershock Following the Main Earthquake. Journal: Modares Civil Engineering Journal, 2024; 24(1). [View at Publisher]

[17] Shome N, Cornell C A. Probabilistic seismic demand analysis of nonlinear structures (Doctoral dissertation). 1999. Stanford University. [View at Google Scholar]; [View at Publisher]

[18] Hisham M, Yassin M. Nonlinear analysis of prestressed concrete structures under monotonic and cycling loads (Doctoral dissertation). 1994. University of California, Berkeley. [View at Google Scholar]; [View at Publisher]

[19] Filippou F C, Popov E P, Bertero V V. Effects of bond deterioration on hysteretic behavior of reinforced concrete joints (Report No. EERC 83-19). 1983. Earthquake Engineering Research Center, University of California, Berkeley. [View at Google Scholar]; [View at Publisher]